Microchemical Journal 106 (2013) 95–101

Contents lists available at SciVerse ScienceDirect

Microchemical Journal

journal homepage: www.elsevier.com/locate/microc

Determination of tributyltin at parts-per-trillion levels in natural waters by second-order multivariate calibration and fluorescence spectroscopy

Manuel Bravo M. [a,*,1], Luis F. Aguilar [b], Waldo Quiroz V. [a], Alejandro C. Olivieri [c,1], Graciela M. Escandar [c,1]

[a] Laboratorio de Química Analítica y Ambiental, Instituto de Química, Pontificia Universidad Católica de Valparaíso, Avenida Brasil 2950, Valparaíso, Chile
[b] Laboratorio de Fotofísica y Espectroscopia Molecular, Instituto de Química, Pontificia Universidad Católica de Valparaíso, Avenida Brasil 2950, Valparaíso, Chile
[c] Departamento de Química Analítica, Facultad de Ciencias Bioquímicas y Farmacéuticas, Universidad Nacional de Rosario e Instituto de Química Rosario (CONICET), Suipacha 531, Rosario (2000), Argentina

ARTICLE INFO

Article history:
Received 21 March 2012
Accepted 22 May 2012
Available online 26 May 2012

Keywords:
Tributyltin
Natural samples
Multivariate calibration
Fluorescence spectroscopy

ABSTRACT

This work presents a non-sophisticated approach for the trace determination of tributyltin, the most toxic organotin species, in very interfering environments, combining fluorescence measurements of its morin complex and the selectivity of second-order chemometric algorithms. The power of MCR–ALS (multivariate curve resolution/alternating least-squares) to quantify tributyltin through fluorescence excitation–emission matrices in the presence of its main degradation products and of a pool of additional twenty-three metal ions is demonstrated. The applied algorithm successfully faces the challenge of solving the strong overlapping among the spectra of the several sample components. The proposed methodology was applied to tap, river, lagoon and seawater spiked samples, obtaining satisfactory results at ng L^{-1} levels, after a pre-concentration step on a C18 membrane, demonstrating the analytical potential of the proposed methodology.

1. Introduction

Due to its widespread use as an antifouling agent in boat paints, highly toxic tributyltin (TBT) is a common contaminant of marine and freshwater ecosystems [1,2]. Exposure to water and sediments contaminated with TBT induces its accumulation on marine biota, and leads to biological effects such as shell malformation in oysters [3], mortality of mussel larvae [4], and imposex of gastropods [5] Potential harmful effects on human health may also result from consumption of contaminated seafood or drinking water [6]. For these reasons, several constraints have been imposed to TBT industrial applications, and the European Union has decided to specifically include TBT compounds in its list of priority compounds in water [7]. Unfortunately, present and future restrictions will not immediately remove TBT and its degradation products, monobutyltin (MBT) and dibutyltin (DBT) from aquatic environments since these compounds are retained in the sediments where they persist [7,8].

Several analytical methodologies have been proposed to quantify organotin compounds, most of them requiring hyphenated techniques, involving a combination of extraction, separation and detection steps [9]. Various pre-concentration procedures have been proposed based on liquid–liquid extraction [10,11], solid-phase extraction (SPE) [12], solid-phase micro-extraction [13,14] and liquid-phase micro-extraction [15,16]. Following this analytical phase, most reported methods combine a separation technique such as gas chromatography (GC) with detection including atomic absorption spectrometry, flame photometry, pulsed flame photometry or inductively coupled plasma mass spectrometry [7,9]. In the case of GC, an additional derivatization step must be included, in order to transform organotins into volatile and thermally stable compounds. Although the analytical performance of these methodologies is widely recognized, allowing the analysis of complex samples containing several unknown components and interferences, they are complex, require a substantial experimental work and skilled analysts, and are difficult to implement for routine analysis.

Modern multivariate calibration methods, especially those based on second-order calibration, constitute an attractive alternative to cope with these situations, even when the processed instrumental data arise from analytical techniques which are intrinsically less selective than chromatography [17]. Certain second-order multivariate algorithms have the property of predicting the concentration of an individual component in the presence of any number of unsuspected constituents, a property commonly named as 'second-order advantage' [18,19]. Usual algorithms employed to analyze second-order data achieving this property are parallel factor analysis (PARAFAC) [20], multivariate curve resolution-alternating least squares (MCR–ALS) [21,22] and some latent-structured methods, such as unfolded partial least-squares (U-PLS) [23] and multiway PLS [24], both combined with residual bilinearization [25,26]. These chemometric methods have been scarcely used for organotin speciation analysis in environmental samples. Only a single work devoted to the quantitation of triphenyltin in seawaters has been reported [27]. However,

* Corresponding author. Tel.: +56 32 2274916; fax: +56 32 2274939.
E-mail address: manuel.bravo@ucv.cl (M. Bravo M.).
[1] The authors contributed equally to the manuscript.

0026-265X/$ – see front matter © 2012 Elsevier B.V. All rights reserved.
doi:10.1016/j.microc.2012.05.013

this latter method does not include TBT as analyte, and only seawater matrices were evaluated.

In the present report, a new analytical method is proposed for quantitation of TBT, which is the most toxic organotin [28–30], based on the measurement of excitation–emission fluorescence matrices (EEFMs) processed by second-order multivariate calibration based on MCR–ALS. Fluorescent detection is possible thanks to the reaction between tributyltin and 3,5,7,2′,4′-pentahydroxyflavone (morin) in a Triton X-100 micellar medium, which yields a fluorescent complex. The feasibility of determining TBT in real matrices is demonstrated by applying the proposed methodology to tap, river, lagoon and sea water samples.

2. Experimental

2.1. Apparatus

Fluorescence measurements were performed on an Aminco Bowman (Rochester, NY, USA) Series 2 luminescence spectrometer equipped with a 150 W xenon lamp and using 1.0 cm path length quartz microcells and slit widths of 4 nm for both monochromators. All measurements were performed at 20 °C with a thermostated cell.

The excitation–emission fluorescence matrices were collected exciting samples in the range of 380–460 nm (each 5 nm) and obtaining the corresponding emission spectra in the range of 510–600 nm (each 5 nm), resulting in a data matrix size 19×17 for sample.

All glassware was rinsed with deionized water, decontaminated overnight in a 20% (v/v) nitric acid solution (Merck, Darmstadt, Germany) and then rinsed again with deionized water.

2.2. Reagents and standards

High quality water (18 MΩ) obtained from a Barnstead Easypure II (Thermo, Dubuque, MA USA) was used to prepare the solutions. The organotin standards, such as monobutiltin trichloride (MBT, 95%), dibutyltin dichloride (DBT, 96%) and tributyltin chloride (TBT, 96%) were obtained from Sigma-Aldrich (St. Louis, M.O., USA). Stock solutions of these reagents (1000 mg L^{-1} of Sn) were prepared in methanol and stored at −20 °C in the dark. Working standards were obtained by dilution with water. This was done on a weekly basis for solutions containing Sn at 5 mg L^{-1} and daily for solutions containing Sn at 10–100 μg L^{-1}.

An ethanolic solution 4.2×10^{-3} M of morin (Sigma-Aldrich, Munich, Germany) was prepared every day, while a stock solution 8.3% (w/v) of Triton X-100 (Fluka Chemika, Buchs, Switzerland) and a buffer solution pH 4.7 of succinic acid (Merck, Darmstadt, Germany) 0.5 M were prepared weekly.

For metal additions, a Certipur® ICP multi-element standard solution IV was purchased from Merck (Darmstadt, Germany). This standard includes 23 elements (Ag(I), Al(III), B(III), Ba(II), Bi(III), Ca(II), Cd(II), Co(II), Cr(III), Cu(II), Fe(III), Ga(III), In(III), K(I), Li(I), Mg(II), Mn(II), Na(I), Ni(II), Pb(II), Sr(II), Tl(I), Zn(II)) at 1000 mg L^{-1} dissolved in diluted nitric acid.

2.3. Synthetic samples

A set of nine TBT calibration solutions with analyte concentrations was built: eight of them contained equally spaced levels between 0 and 350 μg L^{-1} (based on Sn content). They were prepared adding adequate volumes of the standard solution (5 mg L^{-1}) in a calibrated 10.00 mL vessel. Subsequently, 200 μL of morin solution, 1.0 mL of buffer and 0.84 mL of Triton X-100 solution were added. Finally, completion to the mark was achieved with deionized water and the EEFMs were registered.

For validation, two different sets of solutions were prepared including potential interferences in environmental aqueous samples. The first set involved eight solutions containing random concentrations of TBT and their degradation products DBT and MBT, all in the range of 30–110 μg L^{-1} of Sn. Other organotin compounds, such as Triphenyltin (TPhT) and DPhT, were evaluated but they are not significant fluorescence in presence of morin, according to a previous report [31]. The second set consisted of seven solutions with random concentrations of TBT and metals in the range of 32–90 and 38–120 μg L^{-1}, respectively.

It should be noticed that, if these validation samples were subjected to the pre-concentration procedure described below, the lowest concentrations would have been 500 times lower than those quoted above, i.e., in the order of ng L^{-1}, and compatible with the needs of determining TBT at environmental levels.

2.4. Real samples

Tap and river samples were collected from the Rosario city drinking water system and Paraná River (Santa Fe, Argentina), respectively, while the remaining samples were collected from Curauma lagoon and Baron harbor, both placed in the Province of Valparaiso (Valparaiso, Chile). All samples were filtered using a nylon membrane (0.22 μm) and stored at 4 °C until analysis. TBT concentration was determined by GC with pulsed flame photometric detection [11,32], and was found to be below the detection limit. Therefore, aliquots of these samples were spiked with known amounts of TBT, reaching TBT concentrations ranging between 20 and 120 ng L^{-1}. Solid-phase extraction (SPE) using a C18 extraction membrane (Empore, Supelco, Belleponte, P.A., USA) was applied before sample analysis. The disks were loaded into a 13 mm stainless steel filter syringe kit (Alltech, Deerfield, IL, USA) and placed into a syringe. Prior to sample analysis, the disk was conditioned with methanol. Aliquots of either 100 or 200 mL of aqueous samples were passed through the membrane under vacuum pump, with a flow rate of about 10 mL min^{-1}. After elution of the retained organic compounds with 500 μL of methanol, the solvent was evaporated by using dry nitrogen and reconstituted with 400 μL of the fluorogenic solution. This implies a degree of preconcentration of 250 or 500, depending on the sample volume. Finally, the EEFM was measured for each sample and the TBT concentration was estimated using second-order multivariate calibration.

2.5. Theory

2.5.1. PARAFAC

The theory of PARAFAC is well-known [20]. In some of the presently studied systems, this method was employed to successfully decompose the three-way arrays built with the fluorescence data matrices. However, PARAFAC could not be applied with equal success to samples containing uncalibrated interferents having excitation spectra which are strongly overlapped with those of the calibrated components. This has been previously shown to be a strong challenge to PARAFAC [33,34]. The general problem of second-order calibration under strong profile overlapping in one of the data dimensions can be solved using MCR–ALS, which is thus described in detail in Section 2.5.2.

2.5.2. MCR–ALS

In this second-order multivariate method, an augmented data matrix is created from the test and calibration data matrices. The matrices are all of size $J \times K$, where J is the number of excitation wavelengths and K is the number of emission wavelengths. Augmentation can be performed in either direction, depending on the type of experiment being analyzed and also on the presence of severe overlapping in one of the data modes [18,35]. In the presently studied case, the excitation spectra of some of the various sample components are very similar, and hence it is useful to implement augmentation in this direction, creating a row-wise augmented matrix **D** by

placing the different matrices adjacent to each other. Matrix augmentation in this mode helps to destroy the linear dependency caused by strong profile overlapping, as has been previously described [33,34].

The bilinear decomposition of the augmented matrix is then performed according to the expression:

$$\mathbf{D} = \mathbf{C}\mathbf{S}^{\mathrm{T}} + \mathbf{E} \tag{3}$$

where the columns of **C** contain the excitation profiles of the intervening species, the rows of **S** are the emission spectra in the different samples, and **E** is a matrix of residuals not fitted by the model. Appropriate dimensions of **D**, **C**, **S** and **E** are $J \times (IK)$, $J \times N$, $N \times (KI)$ and $J \times (IK)$, respectively (I is the total number of samples in matrix **D**, and N the number of responsive components). Decomposition of **D** is achieved by iterative least-squares minimization of the Frobenius norm of **E**. The minimization is started by supplying estimated emission spectra for the various components, which are employed to estimate $\hat{\mathbf{S}}$ (with the 'hat' implying an estimated matrix) from Eq. (3):

$$\hat{\mathbf{S}} = \mathbf{D}^{\mathrm{T}}\left(\mathbf{C}^{\mathrm{T}}\right)^{+} \tag{4}$$

where the superscript '+' indicates the generalized inverse. With matrix $\hat{\mathbf{S}}$ from Eq. (4) and the original data matrix **D**, the matrix **C** is re-estimated by least-squares:

$$\hat{\mathbf{C}} = \mathbf{D}\left(\hat{\mathbf{S}}^{\mathrm{T}}\right)^{+} \tag{5}$$

and finally **E** is calculated from Eq. (3) using **D** and the estimated $\hat{\mathbf{C}}$ and $\hat{\mathbf{S}}$ matrices. These steps are repeated until convergence, under suitable constraining conditions during the ALS process, for example, nonnegativity in spectral and time profiles. It is important to point out that MCR–ALS requires initialization with spectral profiles in the emission mode. Several alternatives were evaluated, and the finally selected one depended on the type of analyzed samples. For a set composed of only calibration samples, two chemical components were considered: free morin and the TBT–morin complex, whose spectra were estimated from the corresponding PARAFAC decomposition of the three-way calibration data array. When additional components (unexpected interferents) occurred in the samples, their spectral emission profiles were estimated by PARAFAC decomposition of a three-way array composed of calibration and also from data for the test sample.

After MCR–ALS decomposition of **D**, concentration information contained in **S** can be used for quantitative predictions, by first defining the analyte concentration score as the area under the profile for the ith sample:

$$a(i,n) = \sum_{k=1+(i-1)K}^{iK} S(n,k) \tag{6}$$

where $a(i,n)$ is the score for the component n in the sample i. In this way, the scores are employed to build a pseudo-univariate calibration graph against the analyte concentrations, predicting the concentration in the test samples in the usual univariate manner:

$$\left[a(2,n)|a(3,n)|\ldots|a(I,n)\right] = m_2\mathbf{y}^{\mathrm{T}} + n_2 \tag{7}$$

$$y_{\mathrm{u}} = [a(1,n) - n_2]/m_2 \tag{8}$$

where n indicates the analyte, y_{u} is the predicted concentration, and **y** the vector [size $(I-1)\times 1$] of nominal concentrations in the calibration samples.

2.6. Software

All calculations were carried out using MATLAB 7.0 routines (The Mathworks Inc., 2003). The codes available on the internet for MCR–ALS ([36], http://www.ub.edu/mcr/web_mcr/download.html) and PARAFAC (www.models.kvl.dk/algorithms) were employed for multivariate analysis. PARAFAC was applied through a MATLAB graphical user interface which is also available on the Web ([37]; http://www.chemometry.com/Index/Links%20and%20downloads/Programs.html).

3. Results and discussion

3.1. Optimization of the fluorescence signal

TBT forms stable complexes with several flavones, such as morin and fisetin [31], with morin giving the most intense fluorescence signal. The presently proposed method is based on the reaction between TBT and morin in a Triton X-100 micellar medium to yield a fluorimetrically active complex. The fluorescence emission of the complex is affected by several experimental variables, which were evaluated with a Plackett–Burman design, in accordance with the factor levels presented in Table 1. The evaluated response was the emission of the TBT complex at 550 nm. After statistical analysis of the significance of effects, it was concluded that the pH and the type of acid employed significantly affected the fluorescence emission of the TBT–morin complex (see Table 1). Thus succinic acid was selected. Concerning the pH, a univariate optimization was carried out, and the maximum response was found for pH 4.7, retaining this condition for all experiments. For the non significant factors, the low levels were retained for all experiments.

The overlapping between the fluorescence spectra of free morin and its TBT complex hinders the direct spectrofluorimetric determination of the analyte, and the situation becomes more serious if other potential interferents are present. Therefore, in order to overcome this problem, a chemometric analysis was proposed, testing different second-order algorithms. In a first stage, samples only containing TBT were processed, and more complex samples were subsequently studied.

3.2. Set number 1

With the purpose of building a second-order calibration model, EEFMs were recorded for the calibration samples. This calibration set was first analyzed using PARAFAC, which is one of the most frequently applied second-order algorithm, building a three-way array with data corresponding to the calibration samples only. The analysis revealed the presence of two components, which gave a reasonably low residual error to the PARAFAC model, as well as a reasonable value for the so-called core consistency parameter [38]. The analysis of the scores (relative component concentrations) allowed to establish that these two species correspond to free morin and to the TBT–morin complex, because: (1) an excellent linear correlation between scores and nominal calibration concentrations was obtained

Table 1
Factors considered in the screening study concerning the experimental conditions for maximum intensity of the emission of the TBT–morin complex.

	Levels		Analysis responses	
Factors	−1	+1	Effect[a]	Selected conditions
pH	4.5	5.5	++	4.7
Acid	Succinic acid	Acetic acid	−	Succinic acid
Triton X-100 content (% w/V)	0.70	1.30	ns	0.70
Degassed (N_2)	no	yes	ns	No

[a] 95% confidence. '+' and '−'signs correspond to positive and negative effects, respectively. ns: non significant effect.

Table 2
Prediction and statistical results for TBT in samples with MBT and DBT (set no. 2) and with metal ions (set no. 3) using second-order multivariate calibration.

Set no. 2[a]			Set no. 3[b]		
Nominal ($\mu g\ L^{-1}$)[c]	PARAFAC	MCR–ALS	Nominal ($\mu g\ L^{-1}$)[c]	PARAFAC[d]	MCR–ALS[e]
30	44	25	32	17	33
110	121	121	80	59	74
50	60	52	32	17	28
70	87	78	22	21	24
90	94	100	56	53	55
70	73	72	56	34	44
30	48	36	56	48	66
90	92	83			
RMSEP[d]	12	7		13	6
% REP[e]	17	11		31	14

[a] Samples containing random concentrations of MBT and DBT in the range of 20–100 $\mu g\ L^{-1}$.
[b] Samples containing 23 additional metal ions in the range of 20–120 $\mu g\ L^{-1}$.
[c] Concentrations based on Sn mass.
[d] RMSEP ($\mu g\ L^{-1}$): root mean square error of prediction.
[e] REP (%): relative error of prediction.

for one of the components, ascribed to the TBT–morin complex, and (2) the constancy of the scores for the remaining component, which was thus identified as free morin.

As expected, two components were also detected with the MCR–ALS approach and similar prediction results were obtained for the calibration set.

3.3. Set number 2

TBT degradation products, such as MBT and DBT, can be present in environmental samples. These products do also react with morin, forming fluorescent complexes which may in principle constitute potential interferences, while other organotins such as triphenyltin do not react with fluorescent probe [31]. Therefore, a set of solutions including TBT, MBT and DBT was prepared and evaluated with both studied algorithms. The nominal concentrations are shown in Table 2. It is important to notice that these values are higher than environmental levels of TBT and it can be appear unrealistic. However, after a pre-concentration procedure such as proposed below (see Section 3.5) lowest concentrations in true samples could be reached ($ng\ L^{-1}$), being consistent with environmental levels.

The number of PARAFAC responsive components was selected using the same procedures applied to set no. 1 (calibration samples without unexpected components), allowing to assess that three components were required for samples of set no. 2. Fig. 1A and B shows the excitation and emission loadings retrieved by PARAFAC for a typical sample of this set. In addition to the spectra corresponding to morin and TBT–morin complex observed in the calibration samples, a new profile is clearly detected. This profile is ascribed to a combination of the spectra of the uncalibrated species (i.e., MBT– and DBT–morin complexes), a usual phenomenon when interferent profiles with similar spectra occur [39]. Table 2 shows the prediction results corresponding to the application of PARAFAC to the samples of set no. 2. The root mean square error of prediction (RMSEP) and the relative error of prediction (REP) values indicate rather poor results, suggesting that the trilinear model is not adequate for this data. This phenomenon may occur for a number of reasons, such as: (1) lack of profile reproducibility in chromatography, (2) linear dependency among profiles due to closure, or (3) identical profiles for sample components [17,34,40]. As can be appreciated in Fig. 1A, the excitation profile corresponding to the interference signal strongly overlaps with that of free morin. It may be noticed that this problem cannot be solved by employing any of the PLS/RBL algorithms, as has

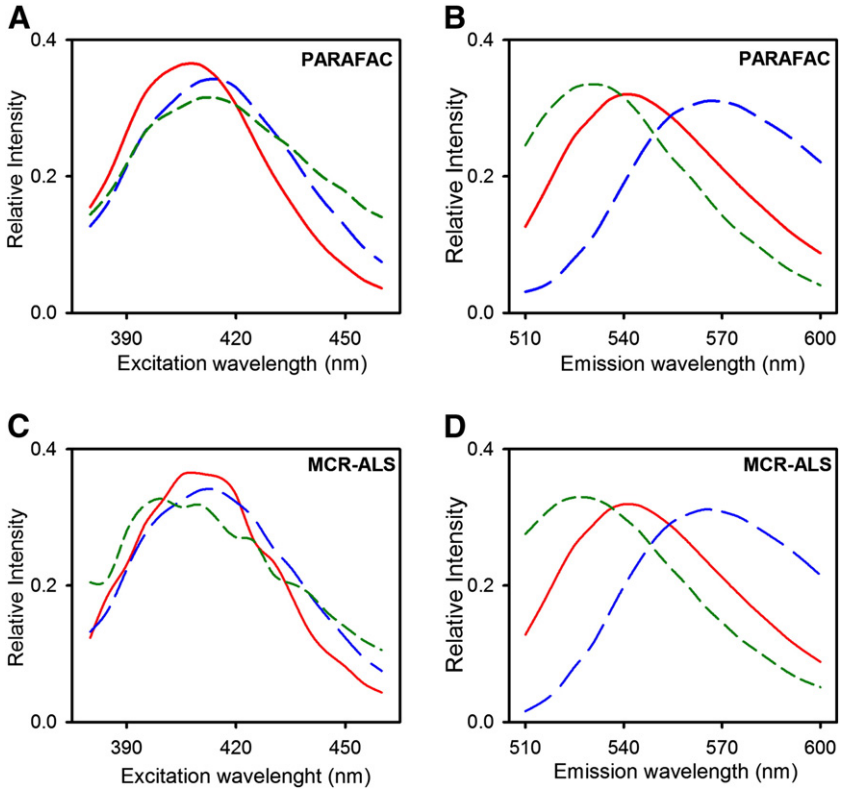

Fig. 1. PARAFAC excitation (A) and emission (B) loadings of free morin (long dashed-blue line), TBT–morin complex (solid-red line) and a combined contribution attributed to both MBT and DBT interferents (short dashed-green line), as obtained for a typical sample from set 2. MCR–ALS excitation (C) and emission (D) loadings of the same components as obtained for the same sample from set 2. Loadings have been normalized to unit length.

been shown for kinetic [33] and lanthanide-sensitized excitation-time decay data [41].

The best alternative for coping with this situation is to apply MCR–ALS in the proper augmentation mode, as explained above. Fig. 1C and D shows the results of the MCR–ALS resolution of excitation-wise augmented data matrix for a typical sample of the same set no. 2, and Table 2 displays the corresponding prediction results of TBT concentration. As can be seen, the results are close to the nominal ones, reaching a REP of 11%. Although it is difficult to assess the limit of detection using MCR–ALS, the results suggest that this figure of merit is around 5 μg L^{-1}, based on the RMSEP values quoted in Table 2. In view of the complexity of the samples and of the analytical problem at hand, the present results are deemed to be reasonably good.

3.4. Set number 3

In coastal impacted sites, seawater samples can contain high levels of metals, such as aluminium, cadmium, lead or zinc [42]. These metal ions, and other potentially present in natural waters, are able to form complexes with morin, which have fluorescence signals overlapped with that of the studied analyte. Therefore, seven test samples containing TBT and 23 inorganic elements other than Sn (see Experimental section) were prepared and evaluated with the PARAFAC and MCR–ALS algorithms. The prediction results for this set are shown in Table 2, and they also indicate a poor performance of PARAFAC. On the other hand, the results given by MCR–ALS are encouraging: the RMSEP and REP values are comparable to those obtained for set no. 2. Based on these values, the limit of detection can presumably be estimated as 5 μg L^{-1}.

The MCR–ALS algorithm retrieved spectra for all sample components which are shown in Fig. 2. In the excitation dimension (Fig. 2A) strong overlapping occurs, which was successfully taken into account by matrix augmentation in this particular dimension. Notice the presence of the interferent in the test sample, and their absence in the calibration samples. This is essential to achieve the second-order advantage.

3.5. Analysis of real aqueous samples

With the purpose of evaluating the application of the present method and the potential interference from background matrices, a recovery study by spiking waters of different origins with TBT was carried out.

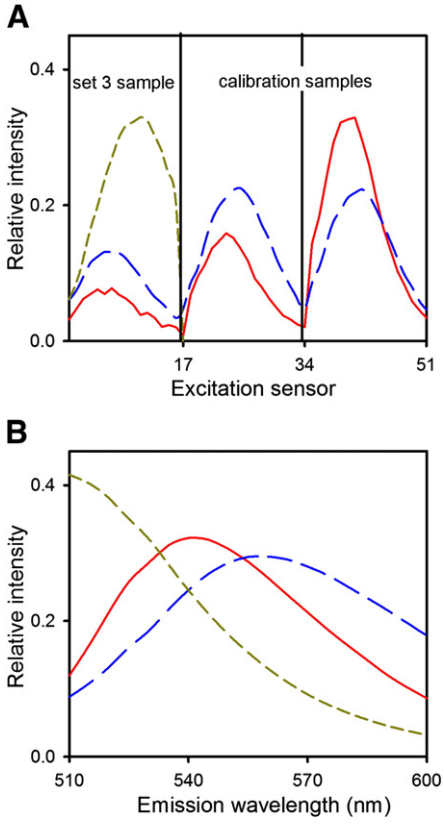

Fig. 2. (A) Excitation spectral profiles of free morin (long dashed-blue line), TBT–morin complex (solid-red line) and a combined contribution attributed to metal–morin complex interferents (short dashed-dark yellow line) obtained after applying MCR–ALS to a typical sample from set 3, and those corresponding to two calibration samples containing analyte concentrations of 25 and 50 μg L^{-1} (as indicated). The vertical lines separate the three samples. (B) Emission profiles obtained after applying MCR–ALS to the same sample of set 3. Loadings have been normalized to unit length.

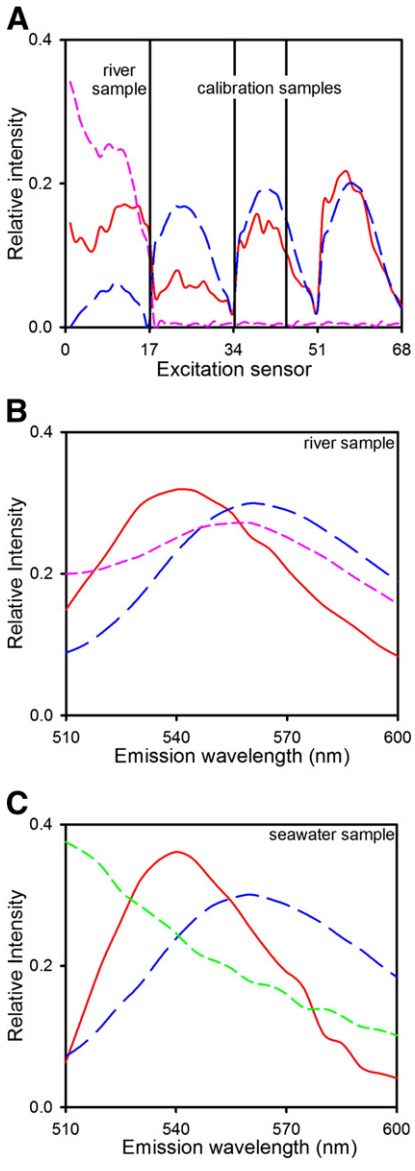

Fig. 3. (A) Excitation spectral profiles of free morin (long dashed-blue line), TBT–morin complex (solid-red line) and unknown interferent (short dashed-pink line) obtained after applying MCR–ALS to a spiked river sample, and those corresponding to three calibration samples containing analyte concentrations of 0, 25 and 50 μg L^{-1} (as indicated). The vertical lines separate the four samples. (B) and (C) Emission profiles obtained after applying MCR–ALS to river and seawater samples, respectively. Short dashed-light green line in (C) corresponds to an unknown interferent in the seawater sample. Loadings have been normalized to unit length.

Before the restrictions on TBT use in antifouling paints, concentrations higher than 500 ng L^{-1} have been detected in North American and European marinas [7]. However, recent investigations have reported that TBT concentrations in water have generally declined, and maximum concentrations in seawater rarely exceed 100 ng L^{-1}. Some countries have set an environmental quality standard for TBT of 20 ng L^{-1} for fresh water [43]. The US Environmental Protection Agency (US-EPA) has developed acute and chronic criteria recommendations for TBT designed to protect aquatic life (http://water.epa.gov/scitech/swguidance/standards/criteria/aqlife/pollutants/tributyltin/fs-final.cfm. Accessed: October 2011). US-EPA indicates that aquatic life would not be significantly affected if the one-hour average TBT concentration does not exceed 460 and 420 ng L^{-1} in freshwater and saltwater, respectively, more than once every three years on the average (acute criterion), and if the four-day average TBT concentration does not exceed 72 and 7.4 ng L^{-1} in freshwater and saltwater, respectively, more than once every three years on the average (chronic criterion).

As a conclusion, the quantification of TBT in natural waters requires highly sensitive techniques, able to detect concentrations in the order of ng L^{-1}, and therefore these methods usually require pre-concentration steps. The sensitivity of the present method was improved applying solid-phase extraction by employing C18 membranes. The use of these membranes allows us to develop a sensitive, robust and fast method for real matrices.

In view of the above results obtained with synthetic samples, MCR–ALS was the algorithm selected for the present analysis. Fig. 3A and B shows the MCR–ALS decomposition obtained by processing the data matrices of a typical spiked river sample and some standards, and Fig. 3C displays emission profiles corresponding to a seawater sample (the corresponding excitation spectra are very similar to those shown in Fig. 3A). In both of these samples, three chemical species are clearly identified. Two of them correspond to TBT and free morin, whose spectral profiles are reasonably similar to those of the corresponding standards. Interestingly, the remaining spectral profiles may be ascribed to a completely unknown interferent component, absent in the calibration set, but detected by the multivariate calibration method. This demonstrates the high potential of the presently applied chemometric strategy.

The obtained results for different real samples are presented in Table 3. Taking into account the simple sample treatment, the analytical results are reasonably good, with recovery percentages ranging from 85 to 120%. This conclusion is also reflected in Fig. 4, which shows the elliptical joint confidence region for the slope and intercept of the found vs. nominal TBT concentration plot. The ellipse includes the theoretically expected values of (1.0), indicating accuracy of the developed methodology.

Table 3
Recovery study of TBT in spiked real water samples using second-order calibration with MCR–ALS.[a]

Sample	Taken/ng L^{-1}	Found[b]/ng L^{-1}	Recovery/%
Tap water[c]	30	33 (3)	110
	40	39 (4)	98
	60	51 (2)	85
River water[d]	20	22 (1)	110
	80	85 (7)	106
	120	109 (9)	91
Lagoon water[e]	20	24 (1)	120
	70	65 (7)	93
	100	123 (3)	123
Seawater[f]	30	28 (4)	93
	50	49 (10)	98
	65	57.3 (0.5)	88
RMSEP[g]		9	

[a] Concentrations based on Sn mass.
[b] Mean of duplicates. Standard deviation between parentheses.
[c] From Rosario City (Santa Fe, Argentina).
[d] Paraná river (Santa Fe, Argentina).
[e] Curauma lagoon (Valparaiso, Chile).
[f] Baron harbor (Valparaiso, Chile).
[g] RMSEP (ng L^{-1}): root mean square error of prediction.

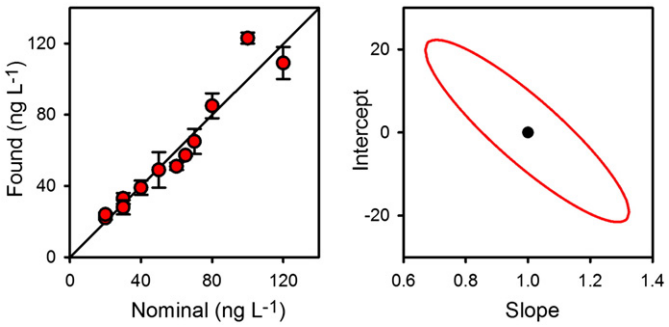

Fig. 4. Plot for TBT predicted concentrations by MCR–ALS in real samples, as a function of the nominal values (the solid line is the perfect fit), and the elliptical joint region (at 95% confidence level) for the slope and intercept of the regression of the data. The black point marks the theoretical (intercept = 0, slope = 1) point.

Based on the average concentration uncertainty which can be measured by the RMSEP in Table 3, the limit of detection for the pre-concentrated water samples can be estimated as ca. 7 ng L^{-1}, which matches the requirements of most official agencies.

The obtained results suggest that interference from the background was successfully removed in the investigated waters by the applied chemometric methodology. Additionally, in the specific case of the seawater samples, the high salt content did not cause difficulties neither in the accuracy nor in the repeatability of the TBT determinations.

4. Conclusions

It has been demonstrated that complexation of tributyltin with morin to form a fluorescent complex, measurement of excitation–emission fluorescence matrix and data processing using multivariate curve resolution/alternating least-squares produce a simple, fast and sensitive method for the determination of tributyltin in aqueous matrices. Through a very simple pre-concentration step with a C18 membrane, it was possible to successfully quantify TBT at part-per trillion levels in environmental water samples. The method represents a valuable alternative for the determination of tributyltin in contaminated water samples.

Acknowledgments

The authors gratefully acknowledge FONDECYT (Project 11080197), CONICET (Project PIP 1950) and ANPCyT (Project PICT 2010-0084). M. Bravo also thanks CONICET-OEA for a postdoctoral fellowship.

References

[1] M. Hoch, Organotin compounds in the environment — an overview, Appl. Geochem. 16 (2001) 719–743.
[2] K. Fent, Ecotoxicological effects at contaminated sites, Toxicology 205 (2004) 223–240.
[3] C. Alzieu, Tributyltin: case study of a chronic contaminant in the coastal environment, Ocean Coast. Manage. 40 (1998) 23–36.
[4] A. Sousa, L. Genio, S. Mendo, C. Barrosoi, Comparison of the acute toxicity of tributyltin and copper to veliger larvae off *Nassarius reticulatus* (L.), Appl. Organomet. Chem. 19 (2005) 324–328.
[5] K.M. Chan, K.M.Y. Leung, K.C. Cheung, M.H. Wong, J.W. Qiu, Seasonal changes in imposex and tissue burden of butyltin compounds in Thais clavigera populations along the coastal area of Mirs Bay, China, Mar. Pollut. Bull. 57 (2008) 645–651.
[6] D.D. Cao, G.B. Jiang, Q.F. Zhou, R.Q. Yang, Organotin pollution in China: an overview of the current state and potential health risk, J. Environ. Manage. 90 (2009) S16–S24.

[7] B. Antizar-Ladislao, Environmental levels, toxicity and human exposure to tributyltin (TBT)-contaminated marine environment. A review, Environ. Int. 34 (2008) 292–308.
[8] S. Diez, M. Abalos, J.M. Bayona, Organotin contamination in sediments from the Western Mediterranean enclosures following 10 years of TBT regulation, Water Res. 36 (2002) 905–918.
[9] R. de Carvalho, R. Erthel Santelli, Occurrence and chemical speciation analysis of organotin compounds in the environment: a review, Talanta 82 (2010) 9–24.
[10] C. Bancon-Montigny, G. Lespes, M. Potin-Gautier, Improved routine speciation of organotin compounds in environmental samples by pulsed flame photometric detection, J. Chromatogr. A 896 (2000) 149–158.
[11] M. Bravo, G. Lespes, I. De Gregori, H. Pinochet, M. Potin-Gautier, Identification of sulfur interferences during organotin determination in harbour sediment samples by sodium tetraethyl borate ethylation and gas chromatography–pulsed flame photometric detection, J. Chromatogr. A 1046 (2004) 217–224.
[12] M. Abalos, J.M. Bayona, R. Compano, M. Granados, C. Leal, M.D. Prat, Analytical procedures for the determination of organotin compounds in sediment and biota: a critical review, J. Chromatogr. A 788 (1997) 1–49.
[13] S. Aguerre, C. Pecheyran, G. Lespes, E. Krupp, O.F.X. Donard, M. Potin-Gautier, Optimisation of the hyphenation between solid-phase microextraction, capillary gas chromatography and inductively coupled plasma atomic emission spectrometry for the routine speciation of organotin compounds in the environment, J. Anal. At. Spectrom. 16 (2001) 1429–1433.
[14] M. Bravo, G. Lespes, I. De Gregori, H. Pinochet, M.P. Gautier, Determination of organotin compounds by headspace solid-phase microextraction-gas chromatography–pulsed flame-photometric detection (HS-SPME–GC-PFPD), Anal. Bioanal. Chem. 383 (2005) 1082–1089.
[15] V. Colombini, C. Bancon-Montigny, L. Yang, P. Maxwell, R.E. Sturgeon, Z. Mester, Headspace single-drop microextration for the detection of organotin compounds, Talanta 63 (2004) 555–560.
[16] H. Shioji, S. Tsunoi, H. Harino, M. Tanaka, Liquid-phase microextraction of tributyltin and triphenyltin coupled with gas chromatography–tandem mass spectrometry — comparison between 4-fluorophenyl and ethyl derivatizations, J. Chromatogr. A 1048 (2004) 81–88.
[17] G.M. Escandar, N.K.M. Faber, H.C. Goicoechea, A.M. de la Pena, A.C. Olivieri, R.J. Poppi, Second- and third-order multivariate calibration: data, algorithms and applications, TrAC, Trends Anal. Chem. 26 (2007) 752–765.
[18] A.K. Smilde, R. Tauler, J. Saurina, R. Bro, Calibration methods for complex second-order data, Anal. Chim. Acta 398 (1999) 237–251.
[19] A.C. Olivieri, Analytical advantages of multivariate data processing. One, two, three, infinity? Anal. Chem. 80 (2008) 5713–5720.
[20] R. Bro, PARAFAC. Tutorial and applications, Chemometr. Intell. Lab. 38 (1997) 149–171.
[21] A. de Juan, R. Tauler, Comparison of three-way resolution methods for non-trilinear chemical data sets, J. Chemometr. 15 (2001) 749–772.
[22] A. de Juan, R. Tauler, Multivariate curve resolution (MCR) from 2000: progress in concepts and applications, Crit. Rev. Anal. Chem. 36 (2006) 163–176.
[23] M.D. Borraccetti, P.C. Damiani, A.C. Olivieri, When unfolding is better: unique success of unfolded partial least-squares regression with residual bilinearization for the processing of spectral-pH data with strong spectral overlapping. Analysis of fluoroquinolones in human urine based on flow-injection pH-modulated synchronous fluorescence data matrices, Analyst 134 (2009) 1682–1691.
[24] S.P. Gurden, J.A. Westerhuis, R. Bro, A.K. Smilde, A comparison of multiway regression and scaling methods, Chemometr. Intell. Lab. 59 (2001) 121–136.
[25] D.B. Gil, A.M. de la Pena, J.A. Arancibia, G.M. Escandar, A.C. Olivieri, Second-order advantage achieved by unfolded-partial least-squares/residual bilinearization modeling of excitation–emission fluorescence data presenting inner filter effects, Anal. Chem. 78 (2006) 8051–8058.
[26] V.A. Lozano, G.A. Ibanez, A.C. Olivieri, A novel second-order standard addition analytical method based on data processing with multidimensional partial least-squares and residual bilinearization, Anal. Chim. Acta 651 (2009) 165–172.
[27] J. Saurina, C. Leal, R. Compano, M. Granados, R. Tauler, M.D. Prat, Determination of triphenyltin in sea-water by excitation–emission matrix fluorescence and multivariate curve resolution, Anal. Chim. Acta 409 (2000) 237–245.
[28] S. Hadjispyrou, A. Kungolos, A. Anagnostopoulos, Toxicity, bioaccumulation, and interactive effects of organotin, cadmium, and chromium on *Artemia franciscana*, Ecotoxicol. Environ. Saf. 49 (2001) 179–186.
[29] K. Fent, Ecotoxicology of organotin compounds, Crit. Rev. Toxicol. 26 (1996) 3–117.
[30] M. Sole, Y. Morcillo, C. Porte, Stress-protein response in tributyltin-exposed clams, Bull. Environ. Contam. Toxicol. 64 (2000) 852–858.
[31] C. Leal, M. Granados, M.D. Prat, R. Compano, Labeling of organotin compounds for fluorometric detection, Talanta 42 (1995) 1165–1170.
[32] N. Mzoughi, G. Lespes, M. Bravo, M. Dachraoui, M. Potin-Gautier, Organotin speciation in Bizerte lagoon (Tunisia), Sci. Total. Environ. 349 (2005) 211–222.
[33] M.J. Culzoni, H.C. Goicoechea, G.A. Ibanez, V.A. Lozano, N.R. Marsili, A.C. Olivieri, A.P. Pagani, Second-order advantage from kinetic-spectroscopic data matrices in the presence of extreme spectral overlapping a multivariate curve resolution — alternating least-squares approach, Anal. Chim. Acta 614 (2008) 46–57.
[34] V.A. Lozano, G.A. Ibanez, A.C. Olivieri, Second-order analyte quantitation under identical profiles in one data dimension. A dependency-adapted partial least-squares/residual bilinearization method, Anal. Chem. 82 (2010) 4510–4519.
[35] R. Tauler, Multivariate curve resolution applied to second order data, Chemometr. Intell. Lab. 30 (1995) 133–146.
[36] J. Jaumot, R. Gargallo, A. de Juan, R. Tauler, A graphical user-friendly interface for MCR–ALS: a new tool for multivariate curve resolution in MATLAB, Chemometr. Intell. Lab. 76 (2005) 101–110.
[37] A.C. Olivieri, H.L. Wu, R.Q. Yu, MVC2: a MATLAB graphical interface toolbox for second-order multivariate calibration, Chemometr. Intell. Lab. 96 (2009) 246–251.
[38] R. Bro, H.A.L. Kiers, A new efficient method for determining the number of components in PARAFAC models, J. Chemometr. 17 (2003) 274–286.
[39] S.A. Bortolato, J.A. Arancibia, G.M. Escandar, Chemometrics-assisted excitation–emission fluorescence spectroscopy on nylon membranes. Simultaneous Determination of benzo[a]pyrene and dibenz[a, h]anthracene at parts-per-trillion levels in the presence of the remaining EPA PAH priority pollutants as interferences, Anal. Chem. 80 (2008) 8276–8286.
[40] A.C. Olivieri, G.M. Escandar, A.M. de la Pena, Second-order and higher-order multivariate calibration methods applied to non-multilinear data using different algorithms, TrAC, Trends Anal. Chem. 30 (2011) 607–617.
[41] V.A. Lozano, R. Tauler, G.A. Ibanez, A.C. Olivieri, Standard addition analysis of fluoroquinolones in human serum in the presence of the interferent salicylate using lanthanide-sensitized excitation-time decay luminescence data and multivariate curve resolution, Talanta 77 (2009) 1715–1723.
[42] C. Barba-Brioso, J.C. Fernández-Caliani, A. Miras, J. Cornejo, E. Galán, Multi-source water pollution in a highly anthropized wetland system associated with the estuary of Huelva (SW Spain), Mar. Pollut. Bull. 60 (2010) 1259–1269.
[43] P. Bermejo Barrera, R.M. Anllo Sendín, M.J. Cantelar Barbazán, A. Bermejo Barrera, Selective preconcentration and determination of tributyltin in fresh water by electrothermal atomic absorption spectrometry, Anal. Bioanal. Chem. 372 (2002) 837–839.